

The value of real-time myocardial contrast echocardiography for detecting coronary microcirculation function in coronary artery disease patients

Lulu Sun, Zilong Wang¹, Tongda Xu*, Defeng Pan*, Li Liang, Ji Hao, Xiaoping Wang*, Dongye Li

Institute of Cardiovascular Disease Research, *Department of Cardiology of Affiliated Hospital of Xuzhou Medical University, Jiangsu Province-P. R. China

¹Department of Cardiology of Affiliated Zhongshan Hospital of Fudan University, Qingpu Branch, Shanghai Municipality-P. R. China

ABSTRACT

Objective: The aim of this study was to evaluate the value of real-time myocardial contrast echocardiography (RT-MCE) for detecting coronary microcirculation (CM) function in coronary artery disease (CAD) patients.

Methods: Sixty-five consecutive patients were divided into CAD (n=52) and no-CAD (n=13) groups using coronary angiography (CAG). All patients underwent RT-MCE at rest and CAG within 1 week after RT-MCE. The ventricular segments in CAD patients were divided semi-quantitatively into ischemic and non-ischemic myocardial groups based on RT-MCE images. Myocardial blood volume (A), myocardial blood flow velocity (β), and mean myocardial blood flow ($A \times \beta$) were obtained. The Gensini scores were calculated for CAD patients. The receiver operating characteristic (ROC) curve areas of A, β , and $A \times \beta$ were calculated to assess CM function in CAD patients.

Results: A total of 798 and 204 segments were investigated in the CAD and non-CAD groups, respectively. In CAD patients, 332 ischemic and 466 non-ischemic segments were identified. The values of A, β , and $A \times \beta$ were significantly different among non-CAD, CAD, ischemic, and non-ischemic groups. ROC curve areas of A, β , and $A \times \beta$ were 0.85, 0.79, and 0.83, respectively, and significant differences were observed in these values among three Gensini score groups of the CAD patients.

Conclusion: Varying degrees of CM function deterioration was observed in CAD patients both in ischemic and non-ischemic areas, with the deterioration being more severe in the former. (*Anatol J Cardiol* 2018; 19: 27-33)

Keywords: real-time myocardial contrast echocardiography, coronary angiography, coronary microcirculation function

Introduction

Coronary microcirculation (CM) function is important in normal cardiac physiology and many disease states. CM dysfunction commonly accompanies epicardial coronary artery lesions (1). Similarly, CM dysfunction has been correlated with anginal syndrome in the case of normal epicardial coronary arteries (Syndrome X). This can result in myocardial infarction, stroke, congestive heart failure, and so on. Many studies have shown CM dysfunction in syndrome X patients (2, 3); however, there are few studies on CM function in CAD patients.

The intracoronary Doppler flow wire or thermodilution technique is considered to be the gold standard for assessing CM dysfunction (4). However, Doppler flow wire is expensive and invasive. Therefore, non-invasive methods, including positron

emission tomography, cardiac magnetic resonance imaging, and real-time myocardial contrast echocardiography (RT-MCE), have become a research focus in this field. Some studies have reported that RT-MCE is consistent with intracoronary Doppler flow in terms of measurements in animals and humans (5–7). As a non-invasive imaging technique, RT-MCE has been validated to be able to visualize microvascular perfusion and to detect perfusion abnormalities (8). It has higher spatial and time resolution and is cheaper, more convenient for bedside operation, and easier to repeat without radioactive contamination. RT-MCE has been used to evaluate microcirculatory dysfunction in patients, including those with cardiac syndrome X (9–11). RT-MCE can be used to evaluate regional myocardial perfusion and coronary microvascular integrity. Nowadays, RT-MCE is conventionally used in clinical practice to detect significant angiographic CAD and to

Address for correspondence: Dongye Li, Institute of Cardiovascular Disease Research, Xuzhou Medical University, Jiangsu Province-P. R. China

Phone: 0516-85582763 Fax: 0516-85582753 E-mail: dongyeli@xzhmu.edu.cn

Accepted Date: 08.11.2017 **Available Online Date:** 29.12.2017

©Copyright 2018 by Turkish Society of Cardiology - Available online at www.anatoljcardiol.com
DOI:10.14744/AnatolJCardiol.2017.8041



assess myocardial viability (12, 13). The parameters calculated from RT-MCE are useful in assessing CM dysfunction with indices, such as A for myocardial blood flow volume (MBV), β for myocardial blood flow (MBF) velocity, and $A \times \beta$ for mean MBF (14, 15). Our study aimed to use RT-MCE to evaluate CM function in CAD patients.

Methods

Patients

Sixty-five consecutive patients (48 men and 17 women) were divided into CAD (n=52) and no-CAD (n=13) groups using coronary angiography (CAG). All patients underwent RT-MCE at rest and CAG within 1 week after RT-MCE. All patients were recruited at the department of cardiology with a considered diagnosis of stable angina pectoris (16). The inclusion criteria were patients over 18 years old with normal left ventricular function on routine echocardiography. Patients who had a history of myocardial infarction, contraindications to the contrast agent, or insufficient acoustic windows on echocardiography were excluded. All candidates underwent in-hospital RT-MCE at rest and CAG.

Ethics statement

The Ethics Committee of the affiliated hospital approved this study. Each patient was enrolled after signing informed consent.

Coronary imaging

CAG was performed in every subject within 1 week after RT-MCE. The results of CAG were analyzed by two experienced interventional cardiologists. The presence of epicardial arteries with >50% diameter stenosis in at least one coronary artery was considered as CAD. The severity of CAD was assessed using the Gensini score; 0 points represent no abnormal findings, 1 point represents <25% degree of stenosis, 2 points represent <50% degree of stenosis, 4 points represent <75% degree of stenosis, 8 points represent <90% degree of stenosis, 16 points represent <99% degree of stenosis, 32 points represent was 100% degree of stenosis. The points were simultaneously obtained for different segments: the points of left main (LM) lesion multiplied by 5, the points of left anterior descending (LAD) branch lesion multiplied by 2.5, the points of LM middle lesion multiplied by 1.5, the points of LM distal lesion multiplied by 1, the points of first diagonal (D1) lesion multiplied by 1, the points of the second diagonal (D2) lesion multiplied by 0.5, the points of left circumflex (LCX) proximal lesion multiplied by 2.5, the points of LCX distal lesion multiplied by 1, and the points of right coronary artery (RCA) lesion multiplied by 1; the sum of each vascular point represents the final points of each patient (17). The results of CAG imaging were analyzed by two experienced interventional cardiologists. If the results were inconsistent, the final consequence for average values was decided by consulting the two cardiologists.

RT-MCE acquisition

The RT-MCE study was performed in all patients using real-time contrast pulse sequencing on an IE33 ultrasound system (Philips IE 33, Philips Medical Systems, Cleveland, OH, USA) with a 1–5-MHz scanning transducer of a low-emitting power preset at a pulse inversion power Doppler mode at a rate of 20–22 frames/s. For the ultrasound contrast agent SonoVue (Bracco, Milan, Italy), 59 mg was dissolved in 5-ml saline, half of which was administered intravenously within 2 min. No side effect was observed in any patient during or after administration. After full myocardial contrast filling, a high-energy pulse mechanical index (1.6) was triggered to destroy the microbubbles and the instrument was turned to a lower energy state of a real-time imaging mechanical index (0.1) to show the microbubble filling process of the myocardial contrast agent. Apical 2-chamber, 4-chamber, and long-axis sections were obtained, and wall-by-wall images were observed to optimize results and avoid artifacts of attenuation and rib shadowing. The machine setting was adjusted to the best state in order to obtain ideal images. When opacification reached a steady state in the cardiac cavity and myocardium, a high mechanical index (1.6) burst (eight frames) of transient microbubble shatter was applied. There was an automatic return to the low mechanical index for continuous imaging of microbubble replenishment for at least 10 cardiac cycles in end-expiration after post-flash. The performance was repeated at least three times in every scan view, and 15 cardiac cycles of every destruction-replenishment sequence were captured and stored as original data.

RT-MCE analysis

The RT-MCE images were analyzed by Q-Lab (version 4.2, Philips Medical Systems, Cleveland, OH, USA) and two experienced physicians who were blinded to the CAG data. The myocardium of the left ventricle was divided into 17 segments according to apical 4-chamber, 2-chamber, and long-axis views (18). The score of semi-quantitative myocardial perfusion analysis was assigned as follow: uniform distribution of contrast as 1, non-uniform distribution of contrast as 0.5, and non-visualization distribution of contrast as 0 (19, 20). Segments with a score of 0.5 on RT-MCE associated with coronary artery stenosis in CAG were defined as ischemic segments. The end-systolic frames (end of T wave) were selected in all cardiac cycles of the replenishment sequence using offline electrocardiographically triggered analysis software (21, 22). The mean signal intensity (SI) was measured automatically at regions of interest (ROIs). The ROIs located in the first post-flash end-systolic frame were copied automatically onto subsequent selected frames and were manually realigned frame-by-frame to maintain a central point within the ventricular wall in the entire replenishment sequence. The segmental SI was plotted against time (t), and the subsequent refilling curve was fitted to the following exponential function: $y(t)=A(1-\exp(-\beta t))+C$, as modified by Wei et al. (23) The segmental MCE parameters, i.e., A for MBV, β for MBF velocity, and $A \times \beta$ for mean MBF, were obtained and

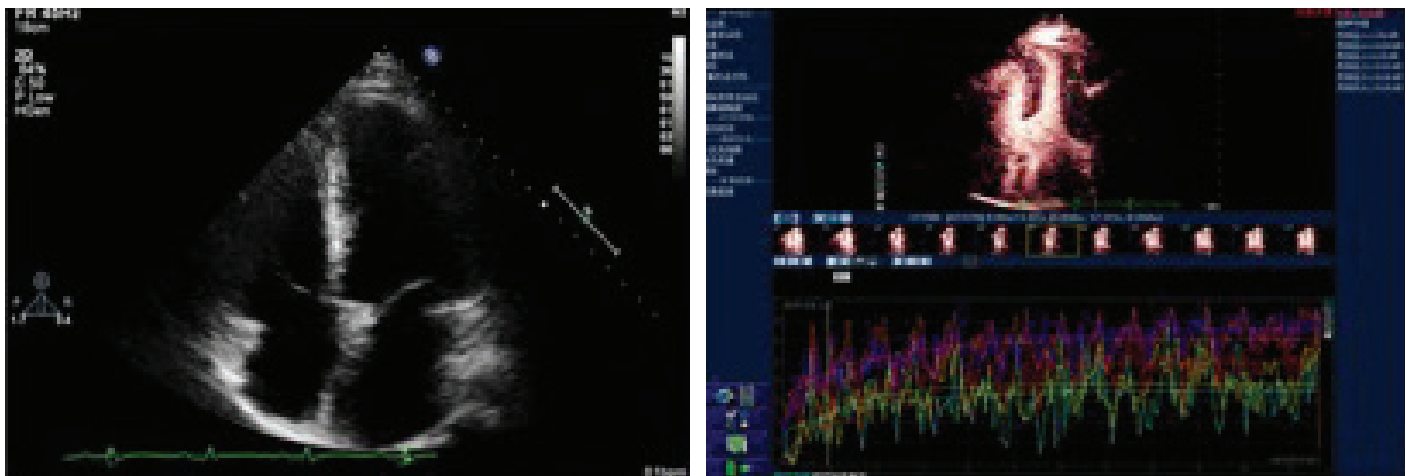


Figure 1. Images of RT-MCE. Picture A represents pre-contrast image, and picture B represents post-contrast image

analyzed for each coronary region (Fig. 1). The measurements of intra-observer variability for A and β were obtained by repeated analysis of 10 randomly selected patients within 8 weeks. The results for MCE parameters were analyzed by two experienced physicians. If the results were inconsistent, the final consequence for average values was decided by two physicians. In addition, the intra- and inter-observer coefficients of variance were calculated.

Statistical analysis

Statistical analyses were performed using SPSS 16.0 (SPSS Inc., Chicago, IL, USA). Continuous variables of baseline clinical

characteristics were expressed as mean±standard deviation (SD). Variables of skewed distribution were expressed as median±interquartile range ($M\pm Q$). Grouped data were compared using non-parametric test. Mann–Whitney U test was used to evaluate continuous data of skewed distribution of two-sample comparison, and X^2 test was used to evaluate categorical data. For more than two groups, Kruskal–Wallis H test was used for proportional comparisons. Correlations among A , β , $A\times\beta$, and Gensini scores were calculated using Kendall correlation analysis. A p value of ≤ 0.05 was considered to be statistically significant. Receiver operating characteristic (ROC) curves were used to evaluate the ability of A , β , and $A\times\beta$ to detect ischemic segments. Intra- and inter-observer variability was presented as the SD of the mean difference (coefficient of variance).

Results

Clinical characteristics and results of CAG

The subjects were divided into CAD patients (52 cases) and non-CAD patients (13 cases). A total of 110 narrow coronary arteries were detected by CAG in the 52 CAD patients. The coronary artery lesions were as follows: 4 vessels in LM, 43 in LAD, 8 in D1, 21 vessels in LCX, 6 in OM, and 28 in RCA. The clinical characteristics of all candidates are listed in Table 1. Of the 52 CAD patients (40 men; mean age, 60.44±8.60 years), 36 had hypertension, 22 had diabetes mellitus, and 20 were current or prior smokers. Of the 13 controls (eight men; mean age, 58.62±7.18 years), six had hypertension, three had diabetes mellitus, and four were current or prior smokers.

RT-MCE

In the 65 study patients, 103 segments were ruled out because of poor image quality. A total of 1002 segments were obtained. In the 52 CAD patients, 86 segments were excluded, and in the 13 non-CAD patients, 17 segments were excluded (Fig. 2). In total, 332 ischemic and 466 non-ischemic segments were detected by semi-quantitative analysis in the CAD patients (Table

Table 1. Baseline clinical characteristics and the data of CAG

Clinical data	CAD patients (n=52)	Non-CAD patients (n=13)
Age, years	60.44±8.60	58.62±7.18
Male	40	8
Risk factors		
Hypertension	36	6
Diabetes	22	3
Smoking	20	4
TC, mmol/L	5.20±1.03	4.01±1.03 ^a
HDL	1.17±0.29	1.21±0.39
Affected arteries		
LM	4 (3.64%)	0 ^a
LAD	43 (39.09%)	0 ^a
D1	8 (7.28%)	0 ^a
LCX	21 (19.09%)	0 ^a
OM	6 (5.45%)	0 ^a
RCA	28 (25.45%)	0 ^a

D1-first diagonal; HDL-C-high-density lipoprotein cholesterol; LAD-left anterior descending; LCX-left circumflex; LM-left main; OM-obtuse marginal; RCA-right coronary artery; TC- total cholesterol; Data are presented as n (%) or mean± SD. ^a $P < 0.05$, CAD vs. non-CAD patients

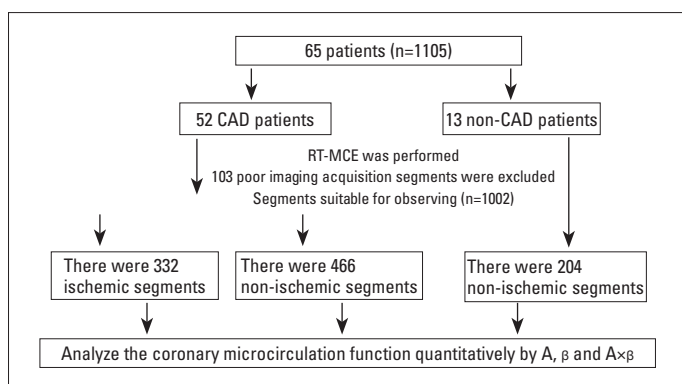


Figure 2. The operation flow chart. In the 65 study patients, 103 segments were ruled out because of poor image quality. A total of 1002 segments were obtained. In the 52 CAD patients, 86 segments were excluded, and in the 13 non-CAD patients, 17 segments were excluded

2). No segment had a score of 0 points because the patients had stable angina pectoris without previous myocardial infarction. On comparison between the CAD and non-CAD groups, significant differences were found in A, β , and $A \times \beta$ (8.78 ± 2.71 , 0.71 ± 0.26 , 5.86 ± 3.57 vs. 3.72 ± 4.33 , 0.39 ± 0.39 , 1.46 ± 3.19 , respectively; $p < 0.001$ for all; Table 3). On comparison between the ischemic and non-ischemic groups of CAD patients, significant differences were observed in A, β , and $A \times \beta$ (3.11 ± 2.11 , 0.33 ± 0.20 , 1.01 ± 1.16 vs. 4.08 ± 5.33 , 0.41 ± 0.41 , 1.60 ± 4.02 , respectively; $p < 0.001$ for all; Table 2; Fig. 3). On comparison between the ischemic and non-CAD groups, significant differences were observed in A, β , and $A \times \beta$ (3.11 ± 2.11 , 0.33 ± 0.20 , 1.01 ± 1.16 vs. 8.78 ± 2.71 , 0.71 ± 0.26 , 5.86 ± 3.57 , respectively; $p < 0.001$ for all; Table 2; Fig. 3). On comparison between the non-ischemic and non-CAD groups, significant differences were found in A, β , and $A \times \beta$ (4.08 ± 5.33 , 0.41 ± 0.41 , 1.60 ± 4.02 , vs. 8.78 ± 2.71 , 0.71 ± 0.26 , 5.86 ± 3.57 , respectively; $p < 0.001$ for all; Table 2; Fig. 3). The intra- and inter-observer coefficients of variance were 94.9% and 92.7% and 95.1% and 93.5% for semi-quantitative and quantitative analyses, respectively.

Gensini scores

For assessing the accuracy of ischemic segments, the ROC curves of A, β , and $A \times \beta$ were 0.85, 0.79, and 0.83, respectively ($p < 0.01$ for all) (Fig. 4). According to the CAG results in the CAD patients, the Gensini scores were 1–29 for the low-risk group, 30–89 for the moderate-risk group, and 90 or higher for the high-risk group. The values of A, β , and $A \times \beta$ were significantly different among the low-, moderate-, and high-risk groups of Gensini

Table 2. A, β , and $A \times \beta$ in CAD and non-CAD groups ($M \pm Q$)

Groups	A	β	$A \times \beta$
Non-CAD group	$8.78 \pm 2.71^{*\Delta}$	$0.71 \pm 0.26^{*\Delta}$	$5.86 \pm 3.57^{*\Delta}$
CAD group	3.72 ± 4.33	0.39 ± 0.39	1.46 ± 3.19
Ischemic group	$3.11 \pm 2.11^{**}$	$0.33 \pm 0.20^{**}$	$1.01 \pm 1.16^{**}$
Non-ischemic group	4.08 ± 5.33	0.41 ± 0.41	1.60 ± 4.02

* $P < 0.001$, Non-CAD vs. CAD group; $^{\Delta}P < 0.001$, Non-CAD vs. Ischemic group; $^{\Delta}P < 0.001$, Non-CAD vs. Non-ischemic group; ** $P < 0.001$, Ischemic vs. Non-ischemic group

scores ($p < 0.001$) (Table 3). A, β , and $A \times \beta$ were significantly different among the three Gensini scores ($p < 0.05$ for all). The values of A and $A \times \beta$ were significantly different between low- and moderate-risk groups as well as between low- and high-risk groups ($p < 0.05$ and 0.01 , respectively). The values of A, β , and $A \times \beta$ were significantly different between moderate- and high-risk groups ($p < 0.05$). The correlation coefficients of A, β , and $A \times \beta$ in the different Gensini score groups were as follows: -0.87 , -0.63 , and -0.90 , respectively, in the low-risk group; -0.85 , -0.77 , and -0.88 , respectively, in the moderate-risk group; and -0.94 , -0.90 , and -0.97 , respectively, in the high-risk group.

Discussion

CM dysfunction is an important mechanism of myocardial ischemia. The advantage of quantitative RT-MCE is the assessment of segmented and total CM function. In this present study, we quantitatively assessed CM function in CAD patients using A, β , and $A \times \beta$. The enrolled patients who successfully underwent CAG were classified into CAD and non-CAD groups. The results showed that CM function in CAD patients was worse than that in non-CAD patients. The myocardial segments of CAD patients were classified semi-quantitatively into ischemic and non-ischemic groups using RT-MCE. CM function in ischemic areas was worse than that in the non-ischemic areas.

Our previous study used RT-MCE combined with dobutamine to detect CAD and viable myocardium; however, we conducted no further study on CM function in CAD patients (24, 25). Ikonomidis et al. (26) assessed the effect of percutaneous coronary intervention in acute coronary syndrome patients by MCE. Shimoni et al. (27) reported the use of MCE to predict its value after revascularization in CAD patients with ventricular dysfunction. However, neither of these studies evaluated CM function in CAD patients. The reasons are as follows: Firstly, the impaired

Table 3. A, β and $A \times \beta$ in Gensini score among low, moderate and high risk groups ($M \pm Q$)

Groups	A	β	$A \times \beta$	Gensini score
Low risk group	3.82 ± 3.61	$0.38 \pm 0.41^{\#}$	$1.32 \pm 3.25^{*\#}$	20.00 ± 20.00
Moderate risk group	$3.35 \pm 3.09^{*\#}$	$0.35 \pm 0.27^{*\#}$	$1.18 \pm 1.75^{*\#}$	$48.00 \pm 29.00^{*\#}$
High risk group	$2.58 \pm 1.20^{***\#}$	$0.30 \pm 0.2^{***\#}$	$0.76 \pm 0.56^{***\#}$	$97.00 \pm 32.00^{***\#}$

* $P < 0.05$, vs. Low risk group; ** $P < 0.01$, vs. Low risk group; $^{\#}P < 0.05$, vs. moderate risk group. $^{\#}P < 0.05$, vs. moderate risk group

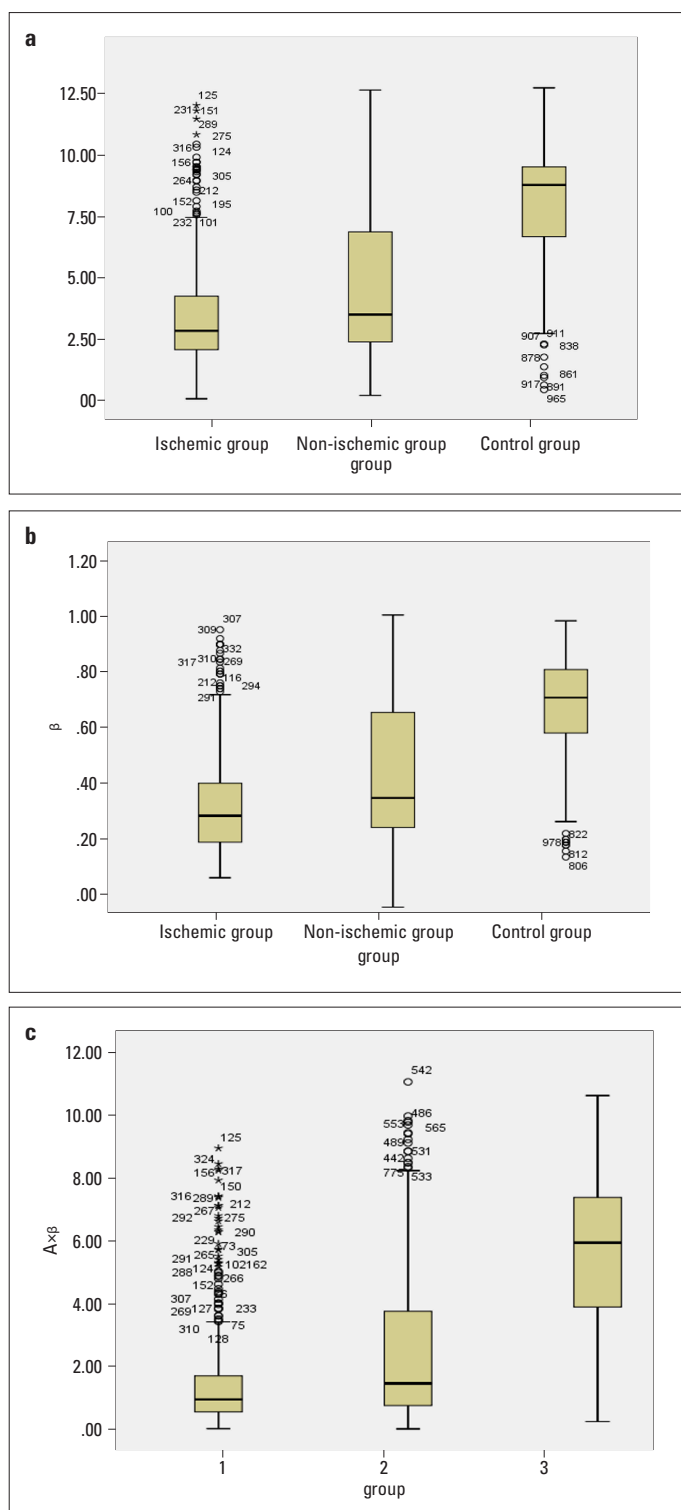


Figure 3. Box plots of A , β , and $A \times \beta$. A (a), β (b), $A \times \beta$ (c) in ischemic, non-ischemic, and non-CAD groups

endothelium dependent or independent release of vasoactive substances resulted in both enhanced microvascular constriction and reduced dilation, which caused functional abnormalities (28). Secondly, non-ischemic regions increase work load to supply and compensate for decreased function in ischemic

areas, and ischemic episodes often break down the structure of the coronary microvasculature, which results in decreased CM function in CAD patients (29–31). Thirdly, coronary artery stenosis can slow blood flow of the epicardial coronary arteries and accelerate local thrombus formation, resulting in decreased CM function in both ischemic and non-ischemic areas of CAD patients (32).

Some animal studies have shown that the ratio of peak stenotic intensity (on behalf of MBV) between narrow and non-narrow coronary artery areas, as measured by the intravenous RT-MCE microbubble technique, positively correlates with the corresponding segments of MBF, as detected by radioactive microspheres. Decreasing MBV and increasing myocardial vascular resistance can result in decreased coronary blood flow in coronary artery stenosis (33). CM function deteriorates when the CM system is affected by one or more adverse factors, such as capillary swelling, congestion, distal embolism, and vasoconstriction (34, 35). These factors result in decreased CM function in CAD by affecting coronary artery endothelial function (36). The similar blood rheology characteristics of red blood cells and good-quality backscatter enable quantitative evaluation of MBF velocity, MBV, and mean MBF in capillaries using microbubbles combined with echocardiographic technology (37). The timing of microbubble refilling in the blood zone supply of narrow coronary arteries is significantly longer than that of normal coronary arteries. RT-MCE has unique capability of assessing myocardial perfusion non-invasively through assessment of capillary blood volume. RT-MCE is a good method for measuring MBF (38).

The Gensini score is a currently recognized method that comprehensively reflects the severity of atherosclerotic vascular lesions (39). It is closely related to the severity and prognosis of CAD. This study found that if the severity of coronary artery lesions was higher, the Gensini score was higher and the parameters of RT-MCE were lower with a negative correlation between them. This suggests that A , β , and $A \times \beta$ can be used to reflect the stenosis degree of coronary artery lesions and CM function. Therefore, RT-MCE can assess CM function in CAD patients.

Study limitations

The most important limitation of our study is the relatively small number of patients in the non-CAD group. Further, the RT-MCE images needed to be analyzed offline and the image quality might have affected the accuracy of the data. We evaluated the CM function of CAD and non-CAD patients using RT-MCE and CAG. CAG is an invasive method, and we did not choose a non-invasive method, such as SPECT, as a reference.

Conclusions

Our results showed that RT-MCE can assess CM function in CAD patients by evaluating myocardial perfusion. There are varying degrees of decrease in CM function in CAD patients in

both ischemic and non-ischemic coronary artery areas, with the decrease in the former being more severe, although CM function deterioration is progressive along with the aggravation of coronary artery stenosis in CAD patients.

Financial support: Jiangsu Clinical Medicine Science and Technology Projects (Grant No. BL2013009); Jiangsu Postgraduate Innovation Pro-ject (Grant No.SJLX15-0721).

Conflict of interest: None declared.

Peer-review: Externally peer-reviewed.

Authorship contributions: Concept – L.S., T.X., D.L., L.L., J.H., Z.W., D.P.; Design – L.S., T.X., D.L., L.L., J.H.; Supervision – T.X., D.L., L.L., J.H., Z.W., D.P.; Fundings – T.X., D.L., D.P.; Materials – L.S., T.X., D.L., L.L., J.H., X.W.; Data collection &/or processing – L.S., L.L., J.H., X.W.; Analysis &/or interpretation – L.S., T.X., D.L.; Literature search – L.S., T.X., D.L., L.L., J.H.; Writing – L.S., T.X., D.L.; Critical review – L.S., T.X., D.L., L.L., J.H., Z.W., D.P., X.W.

References

- Martínez GJ, Yong AS, Fearon WF, Ng MK. The index of microcirculatory resistance in the physiologic assessment of the coronary microcirculation. *Coron Artery Dis* 2015 26 (Suppl 1).
- Marinescu MA, Löffler AI, Ouellette M, Smith L, Kramer CM, Bourque JM. Coronary microvascular dysfunction, microvascular angina, and treatment strategies. *JACC Cardiovasc Imaging* 2015; 8: 210-20.
- Luo C, Long M, Hu X, Huang Z, Hu C, Gao X, et al. Thermodilution-derived coronary microvascular resistance and flow reserve in patients with cardiac syndrome X. *Circ Cardiovasc Interv* 2014; 7: 43-8.
- Claessen BE, Bax M, Delewi R, Meuwissen M, Henriques JP, Piek JJ. The Doppler flow wire in acute myocardial infarction. *Hear* 2010; 96: 631-5.
- Wei K, Ragosta M, Thorpe J, Coggins M, Moos S, Kaul S. Noninvasive quantification of coronary blood flow reserve in humans using myocardial contrast echocardiography. *Circulation* 2001; 103: 2560-5.
- Van Camp G, Ay T, Pasquet A, London V, Bol A, Gisellu G, et al. Quantification of myocardial blood flow and assessment of its transmural distribution with real-time power modulation myocardial contrast echocardiography. *J Am Soc Echocardiogr* 2003; 16: 263-70.
- Zhang WZ, Zha DG, Cheng GX, Yang SQ, Huang XB, Qin JX, et al. Assessment of regional myocardial blood flow with myocardial contrast echocardiography: an experimental study. *Echocardiography* 2004; 21: 409-16.
- Bierig SM, Mikolajczak P, Herrmann SC, Elmore N, Kern M, Labovitz AJ. Comparison of myocardial contrast echocardiography derived myocardial perfusion reserve with invasive determination of coronary flow reserve. *Eur J Echocardiogr* 2009; 10: 250-5.
- Çelik T, Öztürk C, Balta S, Demirkol S, İyisoy A. Coronary microvascular dysfunction in patients with cardiac syndrome X: Ongoing debate. *Int J Cardiol* 2016; 218: 233-4.
- Sucato V, Evola S, Novo G, Corrado E, Coppola G, Andolina G, et al. The association between coronary microvascular dysfunction and carotid intima-media thickness in patients with cardiac syndrome X. *Int J Cardiol* 2016; 214: 383-6.
- Wang N, Li SB, Zhao LS, Li HY, Li ZJ, Shi QW, et al. Relationship between obstructive sleep apnea and coronary microcirculatory function among patients with cardiac syndrome X. *Coron Artery Dis* 2014; 25: 35-9.
- Liu C, Xiu CH, Xiao XG, Ni LX, Liu ZH, Wang BC, et al. Effect of graft patency on the prediction of myocardial viability by dobutamine stress and myocardial contrast echocardiography before coronary artery by-pass surgery. *J Clin Ultrasound* 2014; 42: 9-15.
- Malm S, Frigstad S, Torp H, Wiseth R, Skjarpe T. Quantitative adenosine real-time myocardial contrast echocardiography for detection of angiographically significant coronary artery disease. *J Am Soc Echocardiogr* 2006; 19: 365-72.
- Shimoni S, Frangogiannis NG, Aggeli CJ, Shan K, Quinones MA, Espada R, et al. Microvascular structural correlates of myocardial contrast echocardiography in patients with coronary artery disease and left ventricular dysfunction: implications for the assessment of myocardial hibernation. *Circulation* 2002; 106: 950-6.
- Paraskevaidis IA, Iliodromitis EK, Ikonomidis I, Rallidis L, Hamodrakas E, Parissis J, et al. The effect of acute administration of statins on coronary microcirculation during the pre-revascularization period in patients with myocardial infarction. *Atherosclerosis* 2012; 223: 184-9.
- Athanasiadis A, Sechtem U. Diagnostics and therapy of chronic stable coronary artery disease: new guidelines of the European Society of Cardiology. *European Society of Cardiology. Herz* 2014; 39: 902-12.
- Gensini GG. A more meaningful scoring system for determining the severity of coronary heart disease. *Am J Cardiol* 51: 606
- Senior R, Lepper W, Pasquet A, Chung G, Hoffman R, Vanoverschelde JL, et al. Myocardial perfusion assessment in patients with medium probability of coronary artery disease and no prior myocardial infarction: comparison of myocardial contrast echocardiography with 99 mTc single photon emission computed tomography. *Am Heart J* 2004; 147: 1100-5.
- Leong-Poi H, Le E, Rim SJ, Sakuma T, Kaul S, Wei K. Quantification of myocardial perfusion and determination of coronary stenosis severity during hyperemia using real-time myocardial contrast echocardiography. *J Am Soc Echocardiogr* 2001; 14: 1173-8.
- Lafitte S, Masugata H, Peters B, Togni M, Strachan M, Yao B, et al. Accuracy and reproducibility of coronary flow rate assessment by real-time contrast echocardiography: in vitro and in vivo studies. *J Am Soc Echocardiogr* 2001; 14: 1010-9.
- Yang L, Xia C, Mu Y, Guan L, Wang C, Tang Q, et al. Prognostic Value of Real Time Myocardial Contrast Echocardiography after Percutaneous Coronary Intervention. *Echocardiography* 2016; 33: 421-30.
- Hillis GS, Mulvagh SL, Gunda M. Contrast echocardiography using intravenous octafluoropropane and real-time perfusion imaging predicts functional recovery after acute myocardial infarction. *J Am Soc Echocardiogr* 2003; 16: 638-45.
- Wei K, Jayaweera AR, Firoozan S, Linka A, Skyba DM, Kaul S. Quantification of myocardial blood flow with ultrasound induced destruction of microbubbles administered as a constant venous infusion. *Circulation* 1998; 97: 473-83.
- Li DY, Liang L, Xu TD, Zhang H, Pan DF, Chen JH, et al. The value of quantitative real-time myocardial contrast echocardiography for

- detection of angiographically significant coronary artery disease. *Clin Cardiol* 2013; 36: 468-74.
25. Li DY, Hao J, Xia Y, Zhang H, Xu TD, Wang XP, et al. Clinical usefulness of low-dose dobutamine stress real-time myocardial contrast echocardiography for detection of viable myocardium. *J Clin Ultrasound* 2012; 40: 272-9.
 26. Ikonomidis I, Iliodromitis EK, Tzortzis S, Antoniadis A, Paraskevaidis I, Andreadou I, et al. Staccato reperfusion improves myocardial micro-circulatory function and long-term left ventricular remodeling: a randomized contrast echocardiography study. *Heart* 2010; 96: 1898-903.
 27. Shimoni S, Frangogiannis NG, Aggeli CJ, Shan K, Quinones MA, Espada R, et al. Microvascular structural correlates of myocardial contrast echocardiography in patients with coronary artery disease and left ventricular dysfunction: implications for the assessment of myocardial hibernation. *Circulation* 2002; 106: 950-6.
 28. Arbogast R, Bourassa MG. Myocardial function during atrial pacing in patients with angina pectoris and normal coronary arteriograms. Comparison with patients having significant coronary artery disease. *Am J Cardiol* 1973; 32: 257-63.
 29. Li JS, Zhao XJ, Ma BX, Wang Z. Percutaneous coronary intervention for poor coronary microcirculation reperfusion of patients with stable angina pectoris. *J Biol Regul Homeost Agents* 2016; 30: 733-41.
 30. Layland J, Judkins C, Palmer S, Whitbourn R, Wilson-O'Brien A, MacIsaac A, et al. The resting status of the coronary microcirculation is a predictor of microcirculatory function following elective PCI for stable angina. *Int J Cardiol* 2013; 169: 121-5.
 31. Yong AS, Ho M, Shah MG, Ng MK, Fearon WF. Coronary microcirculatory resistance is independent of epicardial stenosis. *Circ Cardiovasc Interv* 2012; 5: 103-8, S1-2.
 32. Ito H, Maruyama A, Iwakura K, Takiuchi S, Masuyama T, Hori M, et al. Clinical implications of the 'no reflow' phenomenon. A predictor of complications and left ventricular remodeling in reperfused anterior wall myocardial infarction. *Circulation* 1996; 93: 223-8.
 33. Li X, He S, Zhang YS, Chen Y, He JC, et al. Resting Myocardial Contrast Echocardiography for the Evaluation of Coronary Microcirculation Dysfunction in Patients With Early Coronary Artery Disease. *Clin Cardiol* 2016; 39: 453-8.
 34. De Caterina AR, Porto I, Luigi De Maria G, Banning AP. Prevention and treatment of coronary distal embolization in the setting of acute myocardial infarction: pharmacologic approach. *Curr Vasc Pharmacol* 2012; 10: 463-7.
 35. Cuculi F, Herring N, De Caterina AR, Banning AP, Prendergast BD, Forfar JC, et al. Relationship of plasma neuropeptide Y with angiographic, electrocardiographic and coronary physiology indices of reperfusion during ST elevation myocardial infarction. *Heart* 2013; 99: 1198-203.
 36. Takase B, Matsushima Y, Uehata A, Ishihara M, Kurita A. Endothelial dysfunction, carotid artery plaque burden, and conventional exercise-induced myocardial ischemia as predictors of coronary artery disease prognosis. *Cardiovasc Ultrasound* 2008; 6: 61.
 37. Uren NG, Marraccini P, Gistri R, de Silva R, Camici PG. Altered coronary vasodilator reserve and metabolism in myocardium subtended by normal arteries in patients with coronary artery disease. *J Am Coll Cardiol* 1993; 22: 650-8.
 38. Campisi R, Di Carli MF. Assessment of coronary flow reserve and microcirculation: a clinical perspective. *J Nucl Cardiol* 2004; 11: 3-11.
 39. Huang G, Zhao JL, Du H, Lan XB, Yin YH. Coronary score adds prognostic information for patients with acute coronary syndrome. *Circulation* 2010; 74: 490-5.